SAND2024-14228C

Sandia National Laboratories

Enabling Ductile Failure Prediction in Additively Manufactured Metals *via* 3D Characterization

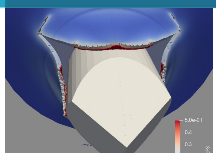

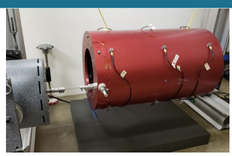

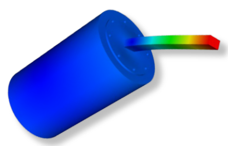

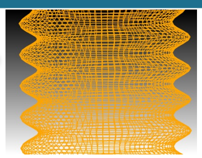

N-O-MAD Research Institute

Paul Chao[1], Ivana Hernandez[2], Thomas Cisneros[3], Suhanna Bamzai[4], Chad Hovey[1], Brian Phung[5], Professor Ashley Spear[5], John Emery[1], Andrew Polonsky[1]

[1]Sandia National Laboratories, [2]University of at Texas El Paso, [3]New Mexico State University, [4]Georgia Institute of Technology, [5]University of Utah

34th Rio Grande Symposium on Advanced Materials
Session: Structural Materials and Failure Mechanisms

Sandia National Laboratories is a multimission laboratory managed and operated by National Technology & Engineering Solutions of Sandia, LLC, a wholly owned subsidiary of Honeywell International Inc., for the U.S. Department of Energy's National Nuclear Security Administration under contract DE-NA0003525.

SAND#

U.S. DEPARTMENT OF ENERGY

NNSA National Nuclear Security Administration

Motivation & Background

- Increasing need for reliability and safety (Ex: Automotive, Healthcare, Aerospace)
- **Additive Manufacturing (AM):**
  - Produces complex geometries with unprecedented design freedom and customization
  - Generates non-uniform material properties, extreme anisotropy, and ***inherent porosity***.

Specimen Build Settings

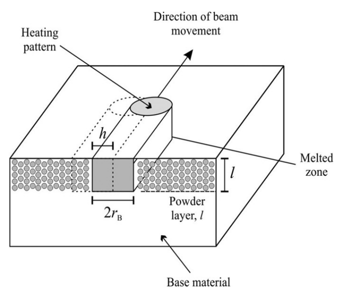

Anisotropic Pores

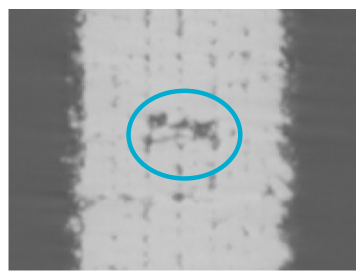

Premature Fracture

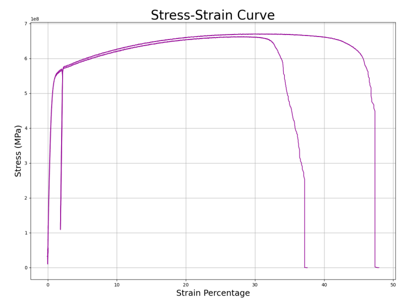

Goal: Validate different failure prediction approaches given the set of experimental data.

- **Prediction model**: Direct Numerical Simulation (DNS): Gold standard of failure prediction.

Experimental Data Overview

Total of 26 316L Additive Manufactured tensile samples

CAD file

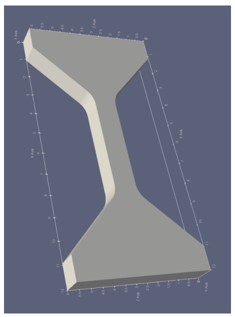

Laser Powder Bed Fusion

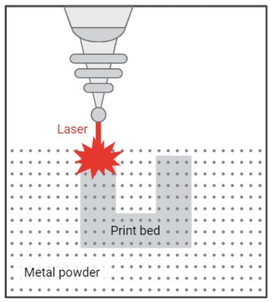

316L SS specimens (26)

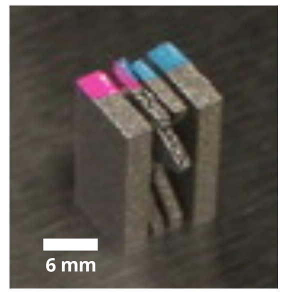

Various Fabrication Parameters

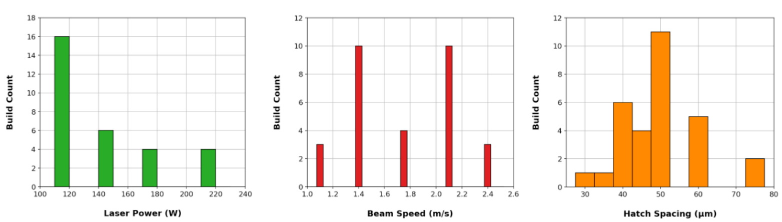

Normalized Energy Calculations

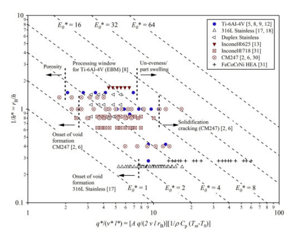

3D Characterization & Mechanical Testing

Micro-CT before and after Fracture

Tensile Testing

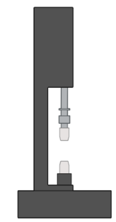

Data Reconstruction

As-Built Samples

Grayscale Segmented

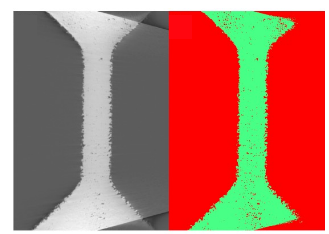

Fractured Samples

Grayscale Segmented

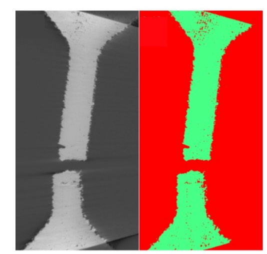

Project workflow

Raw and Segmented Data

As-Built Samples

Grayscale Segmented

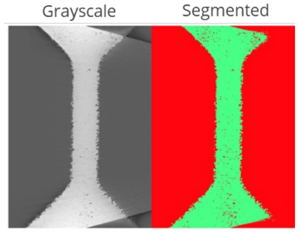

Stress-Strain Data

Stress (MPa)	Strain (%)
26.8918	-0.00402
27.11515	0.001831
27.47726	0.00209
27.78574	0.001993
28.35874	0.001997

Fractured Samples

Grayscale Segmented

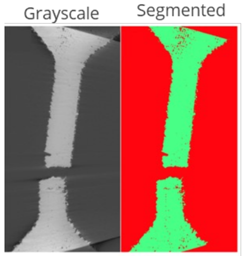

Image and data Pre-processing

Stress-Strain normalization

↓

Crop Data

↓

recon3d
GitLab Repository
Binary to Semantic

↓

Instance Analysis
Pore Processing

↓

Downscale

↓

npy to Mesh

Final Results

Experimental Data Analysis

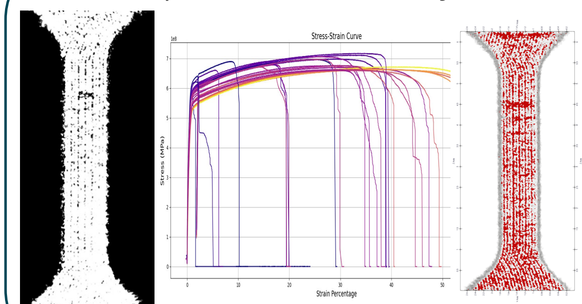

Direct Numerical Simulations (DNS)

Sierra Solid Mechanics

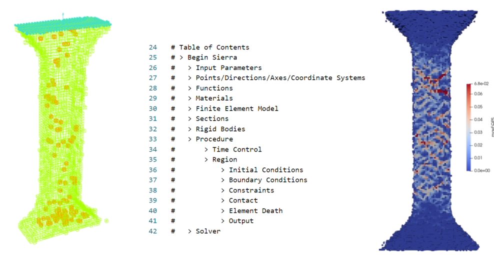

Build settings impact porosity and strength

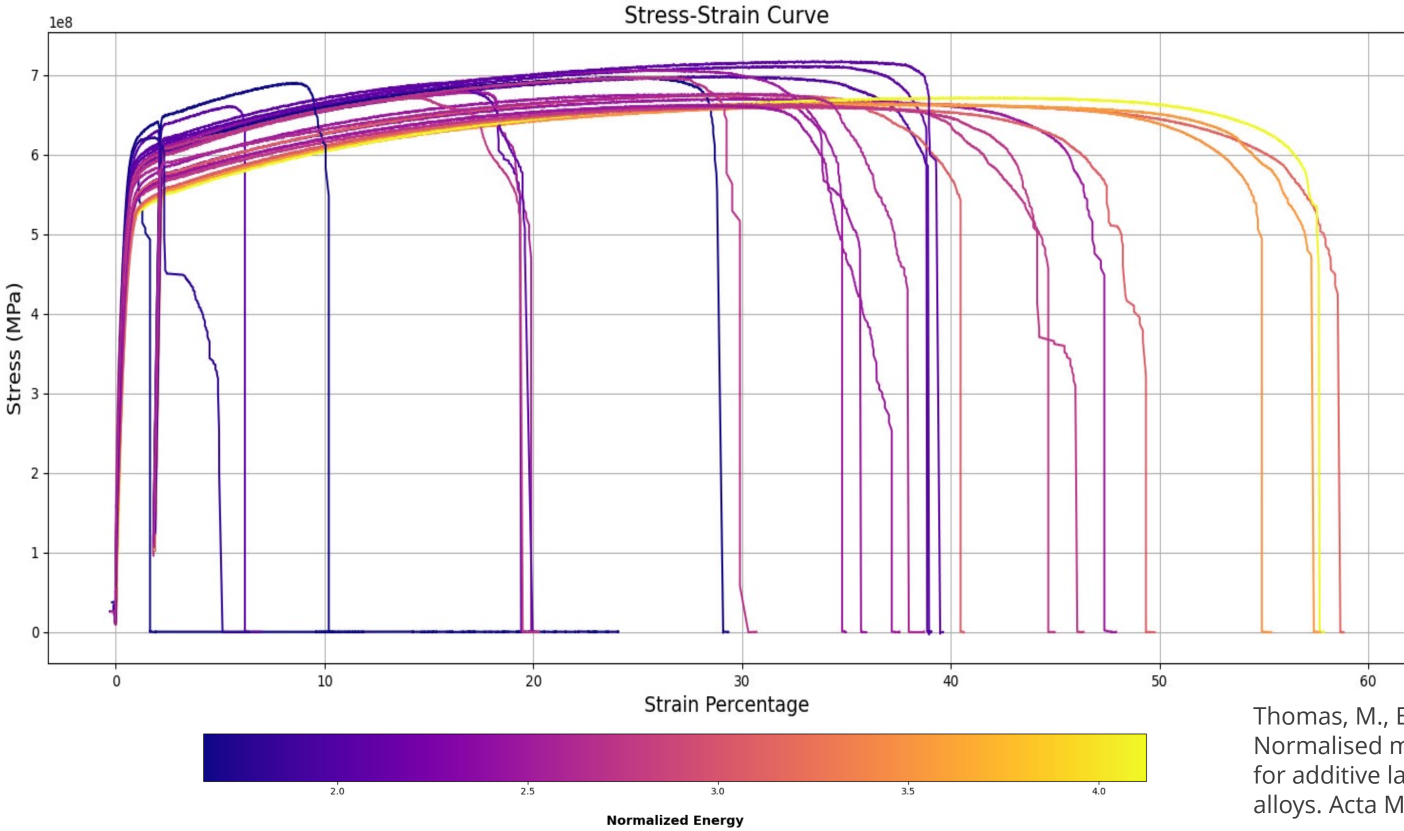

Normalized* Energy

$$E_0^* = \frac{q^*}{(v^*\ h^*\ l^*)}$$

$$q^* = Power$$
$$v^* = Velocity$$
$$l^* = Layer\ height$$
$$h^* = Hatch\ spacing$$

Thomas, M., Baxter, G. J., & Todd, I. (2016). Normalised model-based processing diagrams for additive layer manufacture of engineering alloys. Acta Materialia, Vol. 108, pp. 26–35

Identifying fracture location from experimental data

Fracture location was <u>manually</u> identified with ImageJ using inherent porosity as fiducials

2D cross section | **Reconstruction**

As-Built

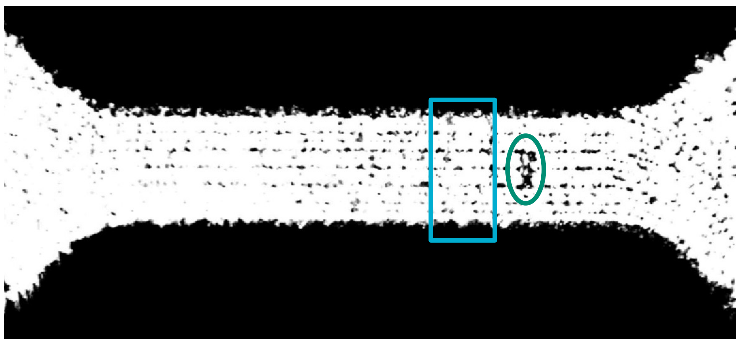

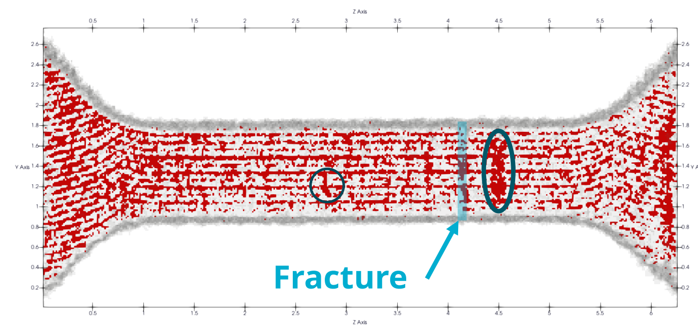

Fractured

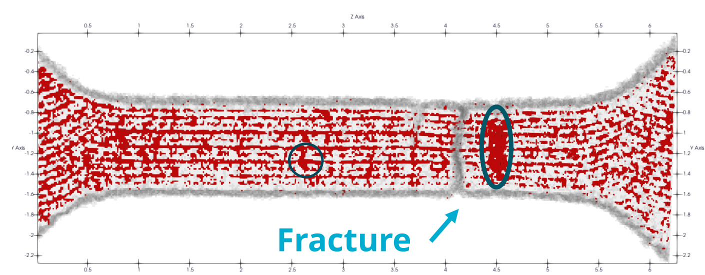

Predicting fracture with direct numerical simulation (DNS)

Mesh creation – voxel size → **Sierra Solid Mechanics simulation workflow** → **Different simulation conditions**

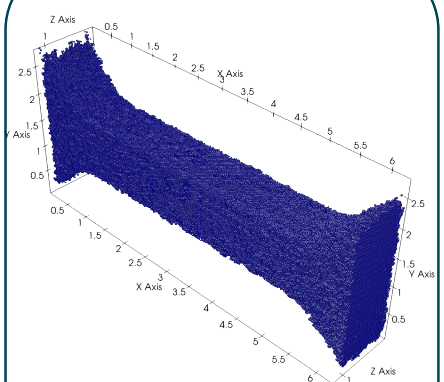

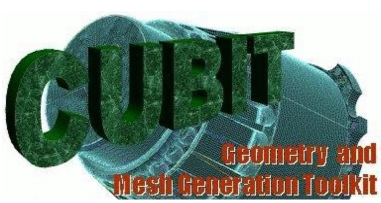

- Hill plasticity model:
  - Anisotropic/rate dependent yield
  - Plasticity captured via Voce hardening
  - Scalar damage model
- Material properties
- Build input deck

Material Property	Variable	Value	Units
Young's Modulus	E	200e9	Pa
Poisson's Ratio	ν	0.27	-
Density	ρ	7920	Kg/m^3
Material Parameter	**Variable**	**Value**	**Units**
Rate independent yield constant	Y_0	453.3e6	Pa
Hill transverse yield ratio	$R_{11} = R_{33}$	1.124	-
Remaining Hill yield ratios	$R_{22} = R_{12} = R_{13} = R_{23}$	1.0	-
Voce hardening coef	A	883.6e6	Pa
Voce hardening exponential coef	b	1.39	-
Yield rate coef	f	21012	$1/s$
Yield rate exponent	n	10.06	-

- Run simulations
- Calibrate parameters

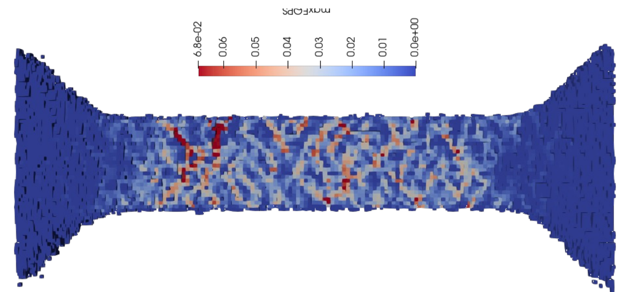

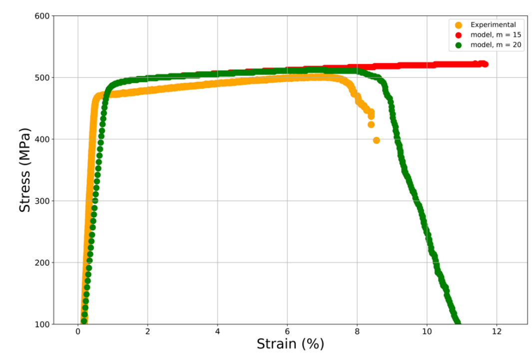

Mesh size limits voxel resolution

80 µm voxel
~13k elements

40 µm voxel
~100k elements

20 µm voxel
~800k elements

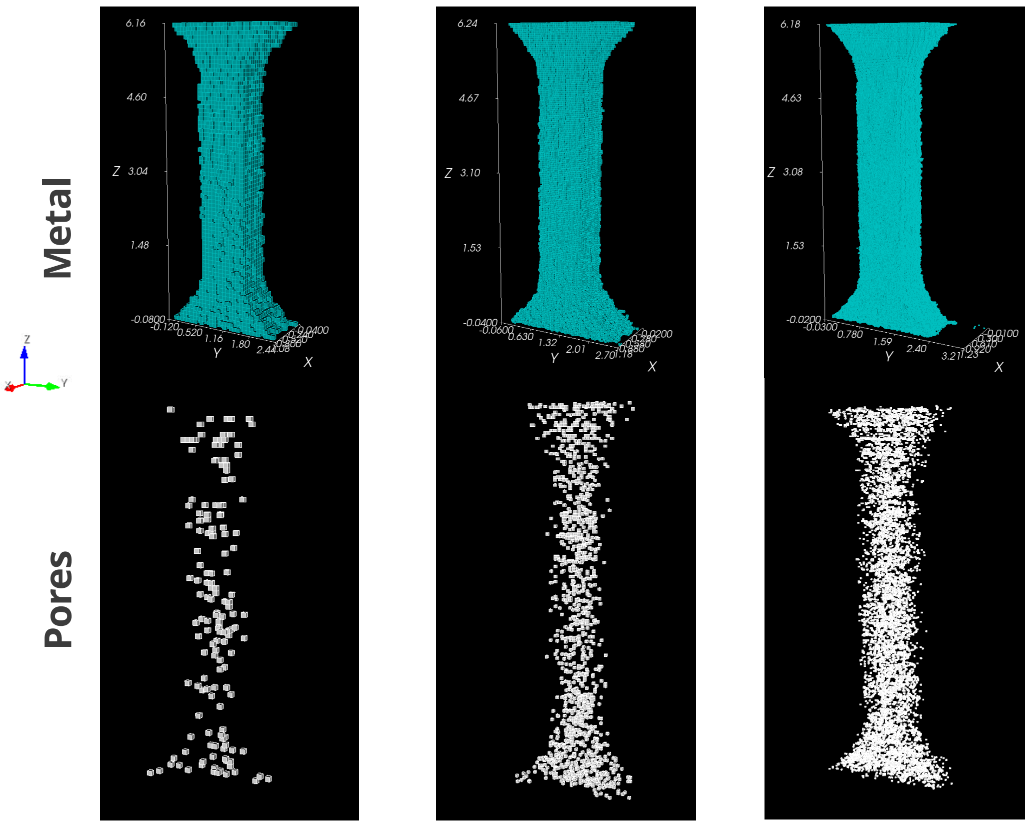

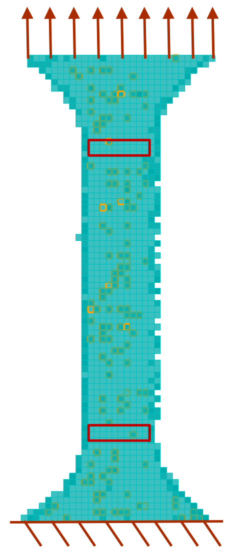

vs.

Experimental CT data
4 µm voxel
>5 million elements
(Impractical to simulate)

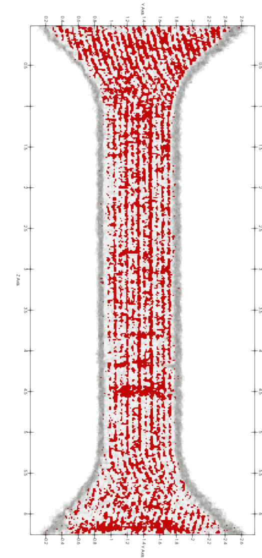

- CUBIT was utilized to add node sets to be used for boundary conditions and remove pore elements.

Direct Numerical Simulation Results

Least Porous

80 μm voxel

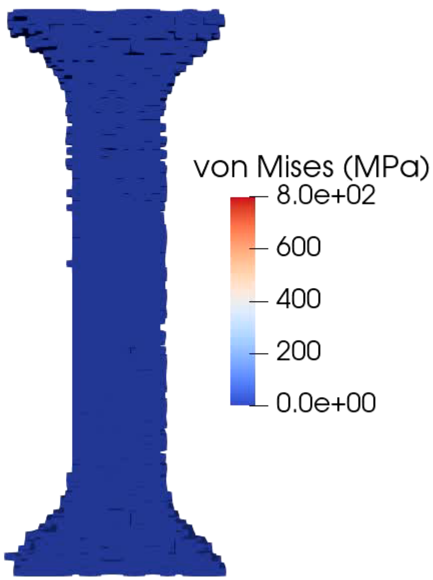

~13k elements
20 processors
0.25 hr wall time

40 μm voxel

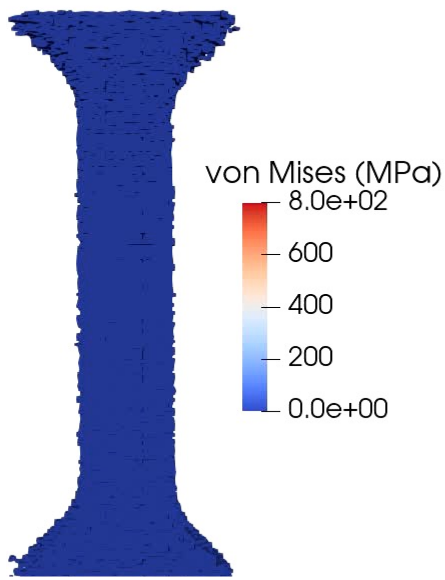

~100k elements
40 processors
1.4 hr wall time

20 μm voxel

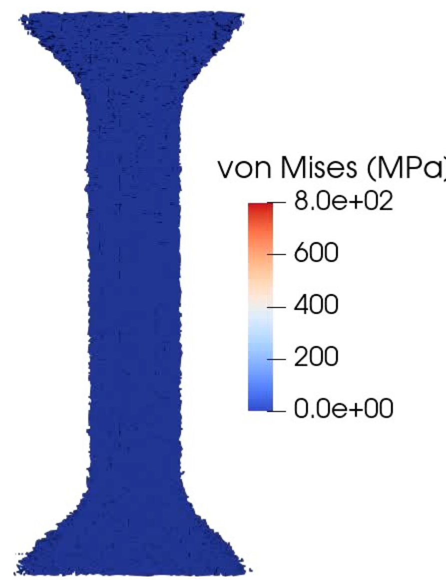

~800k elements
330 processors
2.46 hr wall time

DNS agrees with experimental observations

80 µm voxel

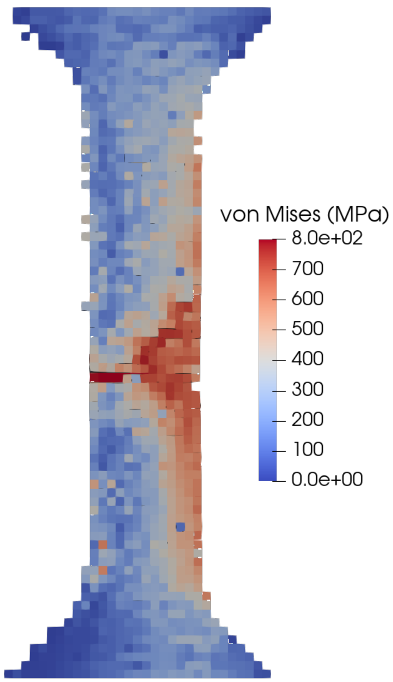

~10k elements

40 µm voxel

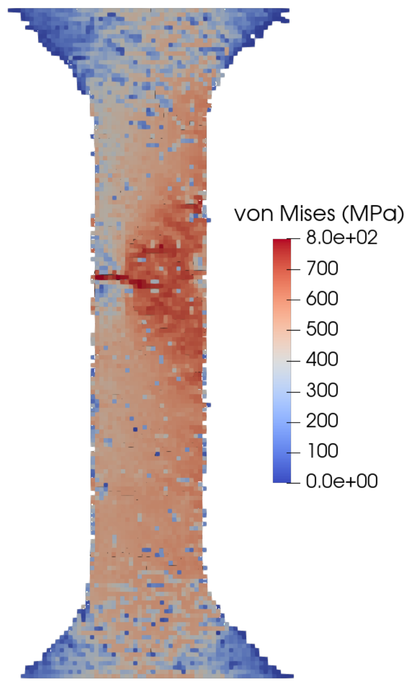

~100k elements

20 µm voxel

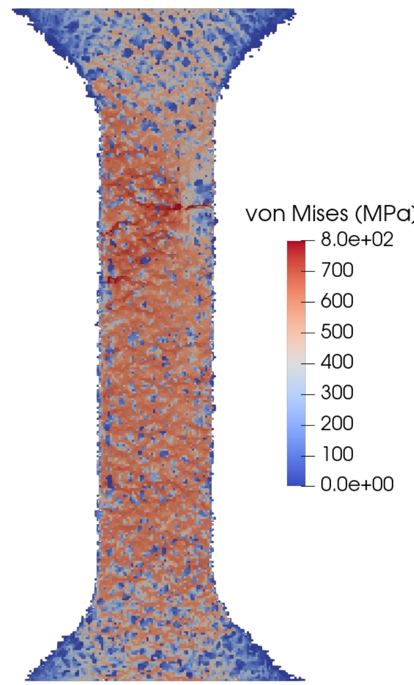

~800k elements

Experimental result (least Porous)

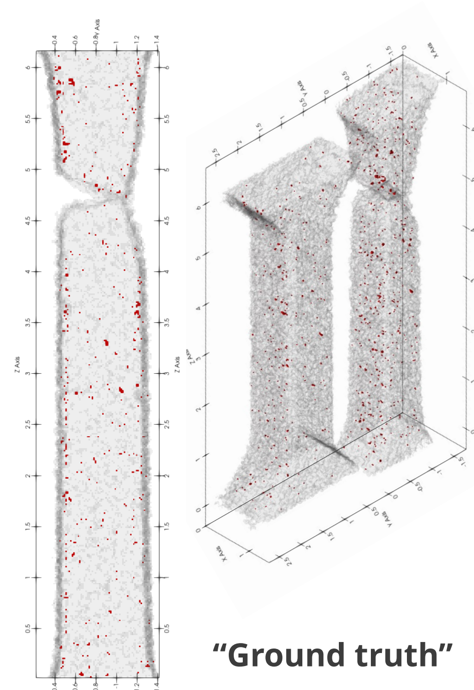

"Ground truth"

Comparing Fracture Locations

Least Porous | Porous | Most Porous

Experiment

Direct Numerical Simulation

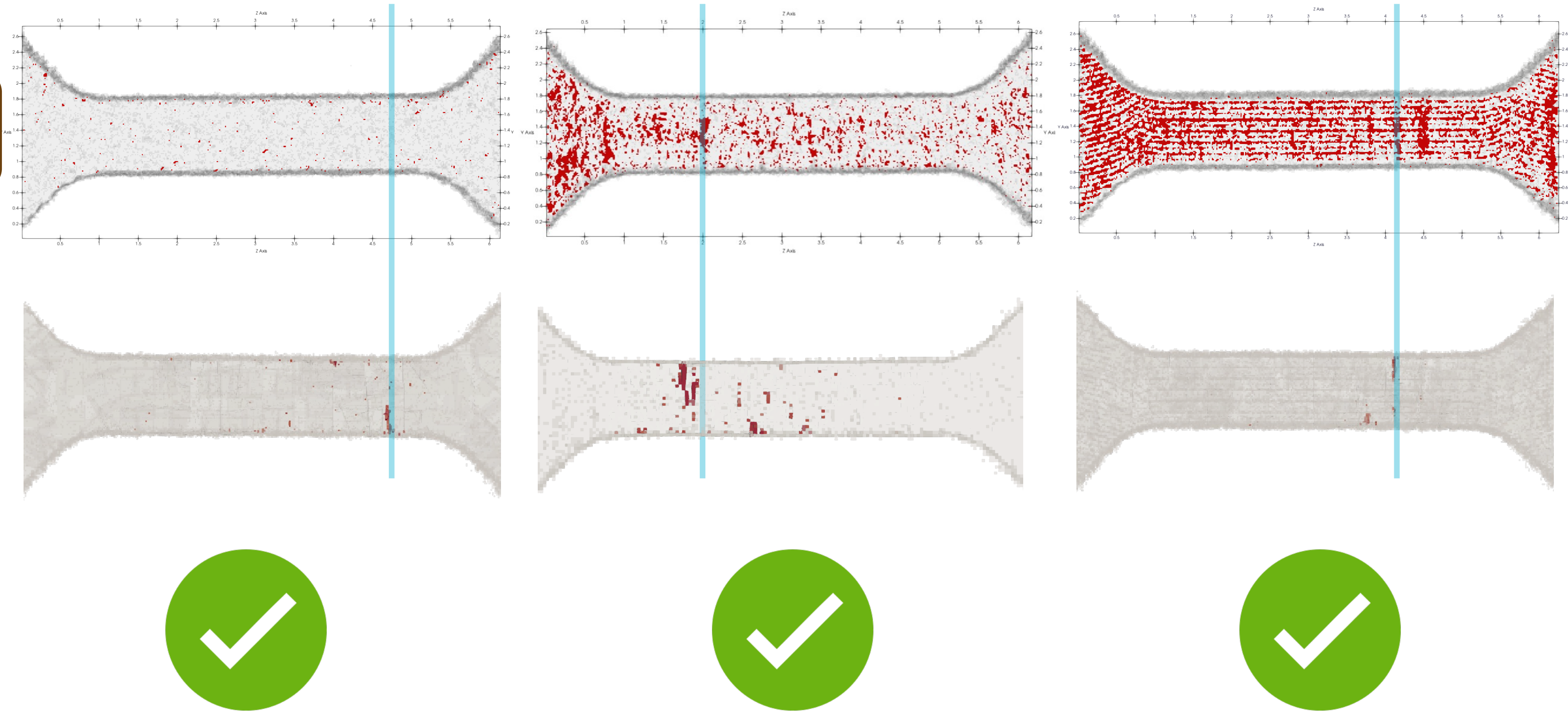

Conclusion

- Preliminary results successfully predict ductile failure in additively manufactured 316L tensile bars with digital twin using Direct Numerical Simulation (DNS) *via* Sierra Solid Mechanics.

Future work

- Compare failure prediction from light-weight, analytical, Void Descriptor Function (VDF) that uses quantitative descriptors of pore geometry and localization effects.

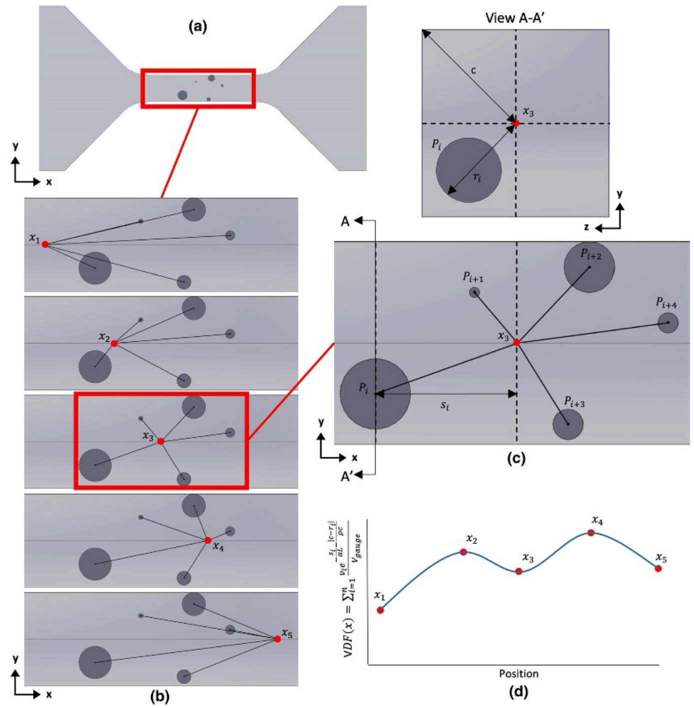

Erickson, J. M., Rahman, A., & Spear, A. D. (2020). A void descriptor function to uniquely characterize pore networks and predict ductile-metal failure properties. In International Journal of Fracture (Vol. 225, Issue 1, pp. 47–67).

Watring, D. S., Benzing, J. T., Kafka, O. L., Liew, L.-A., Moser, N. H., Erickson, J., Hrabe, N., & Spear, A. D. (2022). Evaluation of a modified void descriptor function to uniquely characterize pore networks and predict fracture-related properties in additively manufactured metals. In Acta Materialia (Vol. 223, p. 117464).

THE UNIVERSITY OF UTAH

Acknowledgements

Portions of this research was conducted at the 2024 Nonlinear Mechanics and Dynamics Research (NOMAD) Institute hosted by Sandia National Laboratories and the University of New Mexico.

Ivana Hernandez would like to acknowledge the NNSA Minority Serving Institutions Internship Program (MSIIP) administered by ORISE on behalf of the NNSA for sponsoring her internship at NOMAD.

Sandia National Laboratories is a multimission laboratory managed and operated by National Technology and Engineering Solutions of Sandia, LLC, a wholly owned subsidiary of Honeywell International, Inc., for the U.S. Department of Energy's National Nuclear Security Administration under contract DE-NA-0003525.

Additional Slides

• • •

References

1. Sames, W. J., List, F. A., Pannala, S., Dehoff, R. R., & Babu, S. S. (2016). The metallurgy and processing science of metal additive manufacturing. International Materials Reviews, 61(5), 315–360. https://doi.org/10.1080/09506608.2015.1116649
2. Lewandowski, J. J., & Seifi, M. (2016). Metal Additive Manufacturing: A Review of Mechanical Properties. In Annual Review of Materials Research (Vol. 46, Issue 1, pp. 151–186). Annual Reviews. https://doi.org/10.1146/annurev-matsci-070115-032024
3. Karlson, K. N., Skulborstad, A. J., Madison, J. M., Polonsky, A., & Jin, H. (2023). Toward accurate prediction of partial-penetration laser weld performance informed by three-dimensional characterization – Part II: μCT based finite element simulations. Tomography of Materials and Structures, 2, 100007. https://doi.org/10.1016/j.tmater.2023.100007
4. Bergel, G., Karlson, K., & Stender, M. (2020). Assessing the Influence of Process Induced Voids and Residual Stresses on the Failure of Additively Manufactured 316L Stainless Steel. Office of Scientific and Technical Information (OSTI). https://doi.org/10.2172/1593545
5. Erickson, J. M., Rahman, A., & Spear, A. D. (2020). A void descriptor function to uniquely characterize pore networks and predict ductile-metal failure properties. In International Journal of Fracture (Vol. 225, Issue 1, pp. 47–67). Springer Science and Business Media LLC. https://doi.org/10.1007/s10704-020-00463-1
6. Watring, D. S., Benzing, J. T., Kafka, O. L., Liew, L.-A., Moser, N. H., Erickson, J., Hrabe, N., & Spear, A. D. (2022). Evaluation of a modified void descriptor function to uniquely characterize pore networks and predict fracture-related properties in additively manufactured metals. In Acta Materialia (Vol. 223, p. 117464). Elsevier BV. https://doi.org/10.1016/j.actamat.2021.117464
7. Thomas, M., Baxter, G. J., & Todd, I. (2016). Normalised model-based processing diagrams for additive layer manufacture of engineering alloys. In Acta Materialia (Vol. 108, pp. 26–35). Elsevier BV. https://doi.org/10.1016/j.actamat.2016.02.025
8. E. Voce. (1948). The Relationship Between Stress and Strain for Homogeneous Deformations, J. of the Institute Metals, 74:537-562
9. R. Hill. (1948). A theory of the yielding and plastic flow of anisotropic metals. Proceedings of the Royal Society of London, A193:281-297.

AM 316L SS property specification

- Hill plasticity model:
  - Anisotropic/rate dependent yield
  - Plasticity captured via Voce hardening
  - Scalar damage model

Material Property	Variable	Value	Units
Young's Modulus	E	200e9	Pa
Poisson's Ratio	ν	0.27	-
Density	ρ	7920	Kg/m^3
Material Parameter	**Variable**	**Value**	**Units**
Rate independent yield constant	Y_0	453.3e6	Pa
Hill transverse yield ratio	$R_{11} = R_{33}$	1.124	-
Remaining Hill yield ratios	$R_{22} = R_{12} = R_{13} = R_{23}$	1.0	-
Voce hardening coef	A	883.6e6	Pa
Voce hardening exponential coef	b	1.39	-
Yield rate coef	f	21012	$1/s$
Yield rate exponent	n	10.06	-

Hill plasticity

$$\theta^2(\hat{\sigma}_{ij}) = F(\hat{\sigma}_{22} - \hat{\sigma}_{33})^2 + G(\hat{\sigma}_{33} - \hat{\sigma}_{11})^2 + H(\hat{\sigma}_{11} - \hat{\sigma}_{22})^2 + 2L\hat{\sigma}_{23}^2 + 2M\hat{\sigma}_{31}^2 + 2N\hat{\sigma}_{12}^2$$

Damaged Cauchy stress

$$\hat{\sigma}_{ij} = \sigma_{ij}/(1-\phi)$$

Void volume fraction

Voce Hardening

$$\sigma_f = Y_0\left\{1 + \sinh^{-1}\left[\left(\frac{\dot{\varepsilon}_p}{f}\right)^{1/n}\right]\right\} + A\left((1 - \exp(b\varepsilon_p)\right)$$

Yield

Fitting constant

Fitting exp

[4, 8-9]

Predicting fracture with Void Descriptor Function (VDF)

- Identifies positions along gauge section highly populated by critical pore structures
  - Signals where fracture is likely to occur
- Quantifies the inter-relationships of pores to quickly predict failure
  - Factors: pore location, size, and distance to free surface

Crop Data → Obtain Geometries → Calculate Pore Metrics

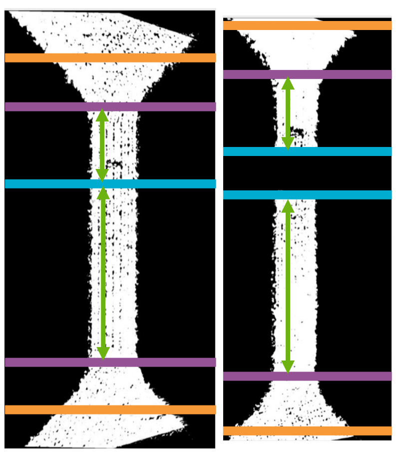

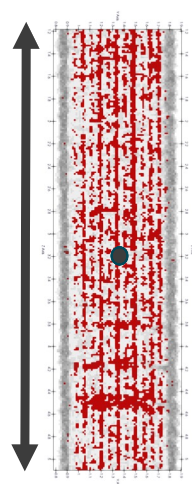

- pores
  - axis_vectors
  - centroids
  - ellipsoid_surface_areas
  - ellipsoid_volumes
  - equivalent_sphere_diameters
  - nearest_neighbor_IDs
  - nearest_neighbor_distances
  - num_voxels
  - semi-axis_lengths

Pre-processing (Image Analysis)

recon3d

GitLab Repository

binary_to_semantic

- Identifies air, pores, and metal independently.
- Converts segmented data (air = 0 & metal = 1) into semantic data, creating three classes:
  - air = 0
  - metal = 1
  - pores = 2
- **Output:** semantic segmentation tiff images.

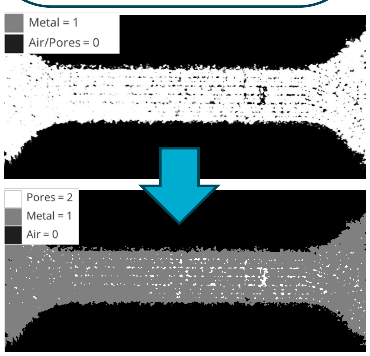

instance_analysis

- Identifies each pore individually
- Provides different pore metrics using semantic data as input.
- **Output:** h5 file with all the information collected from each pore

- pores
  - axis_vectors
  - centroids
  - ellipsoid_surface_areas
  - ellipsoid_volumes
  - equivalent_sphere_diameters
  - nearest_neighbor_IDs
  - nearest_neighbor_distances
  - num_voxels
  - semi-axis_lengths

downscale

- Pads an image stack at a given resolution until it is evenly divisible by a target resolution before downscaling to the target resolution.
- **Output:** downscaled tiff images, a .vtr file, and an .npy file.

Resolution = 4 μm

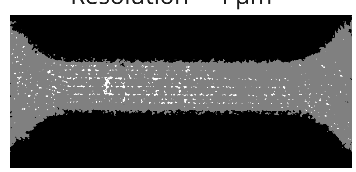

Resolution = 20 μm

npy_to_mesh

- **Input:** .npy file
- **Intermediate outputs:** Creates a Sculpt (.i) input file
- **Output:** Runs Sculpt to create an Exodus (.e) mesh file

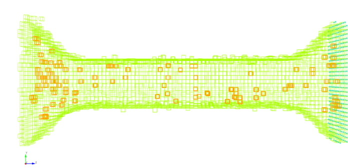

Pore Statistics

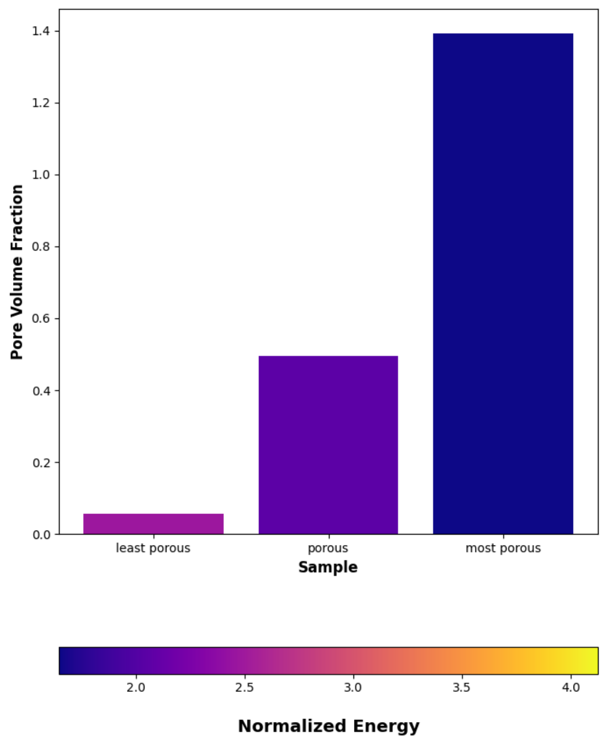

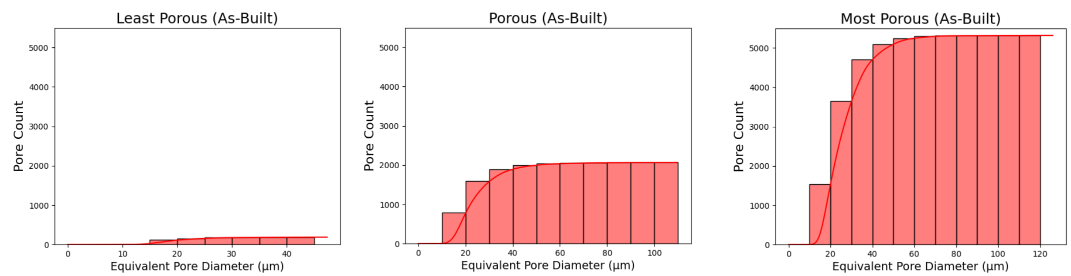

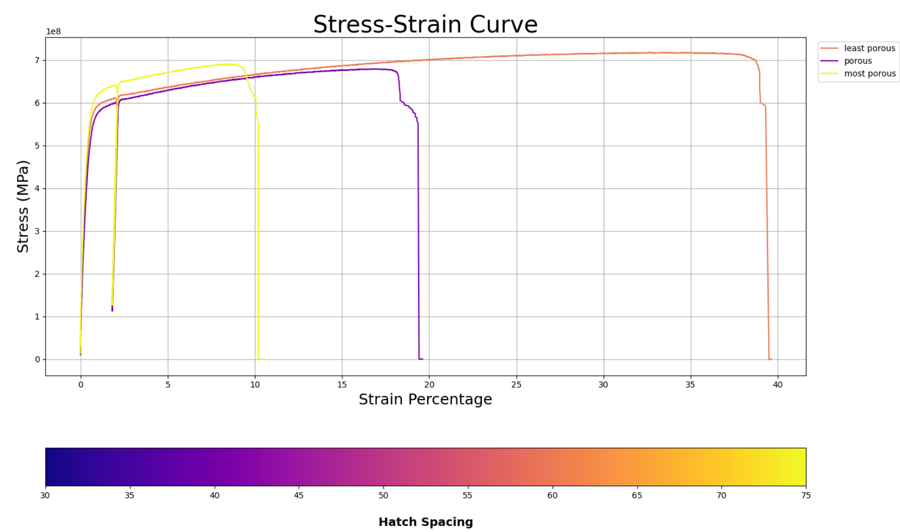

Least Porous Tensile Bar

Least Porous

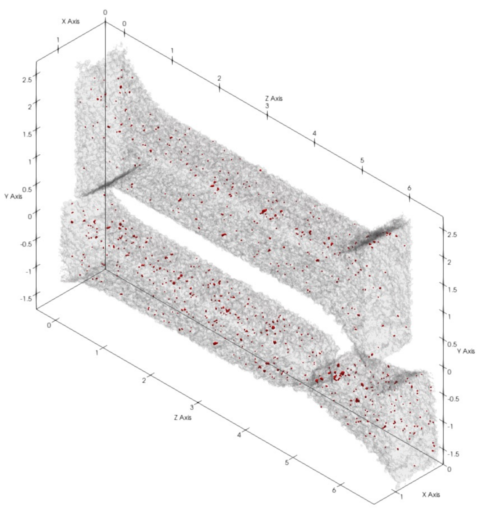

Metal

Pores

Scale is in mm

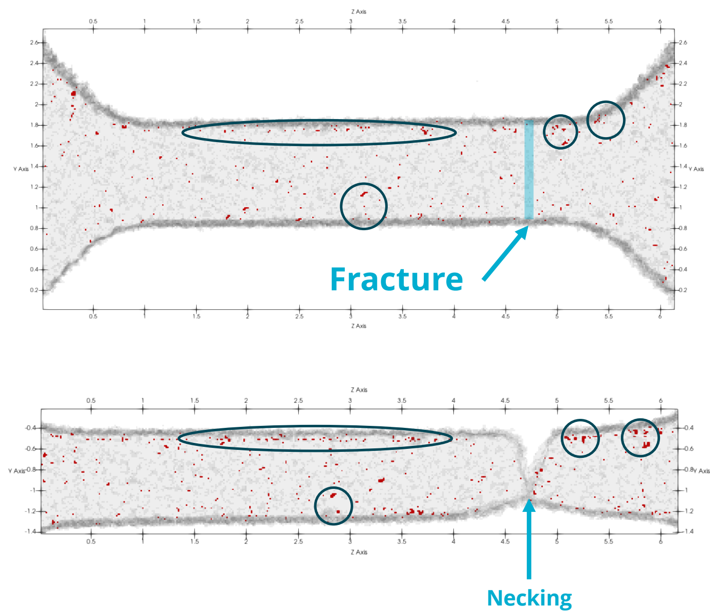

Fracture Location ≈ 4.692 mm

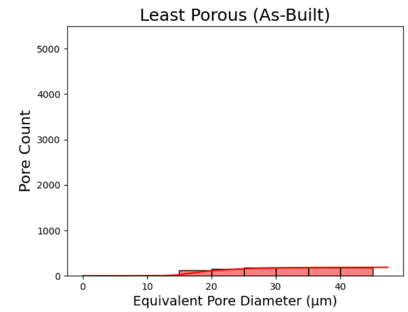

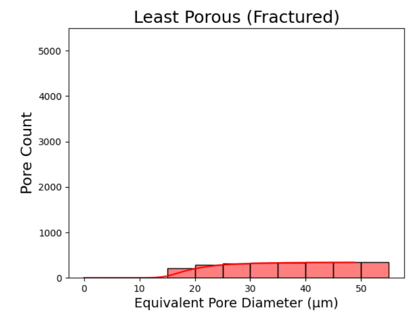

Equivalent diameter 0.22% increase

Porous Tensile Bar

Porous

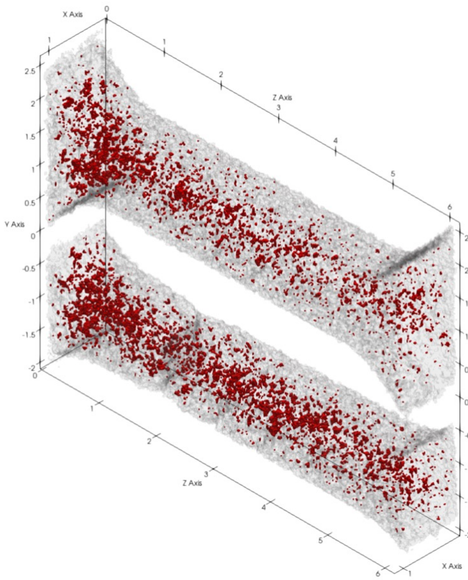

Metal

Pores

Scale is in mm

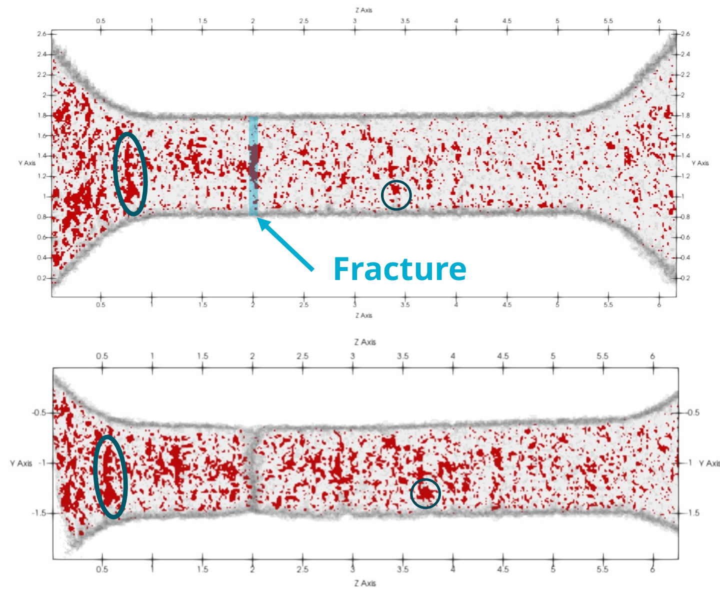

Fracture Location ≈ 2.048 mm

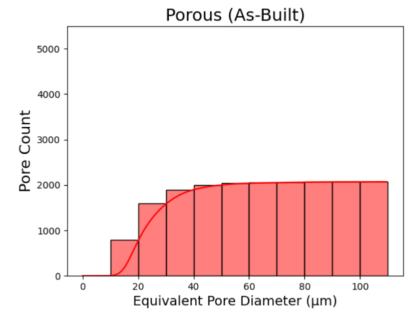

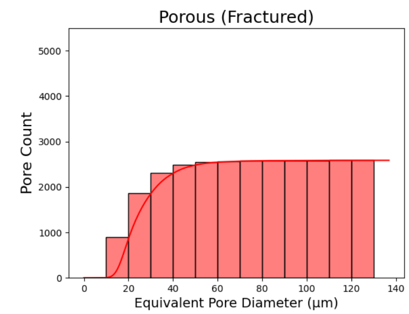

Equivalent diameter 4.36% increase

Most Porous Tensile Bar

Most Porous

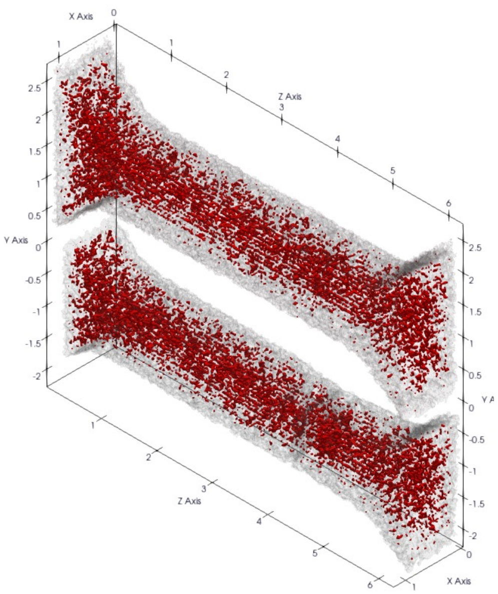

Metal

Pores

Scale is in mm

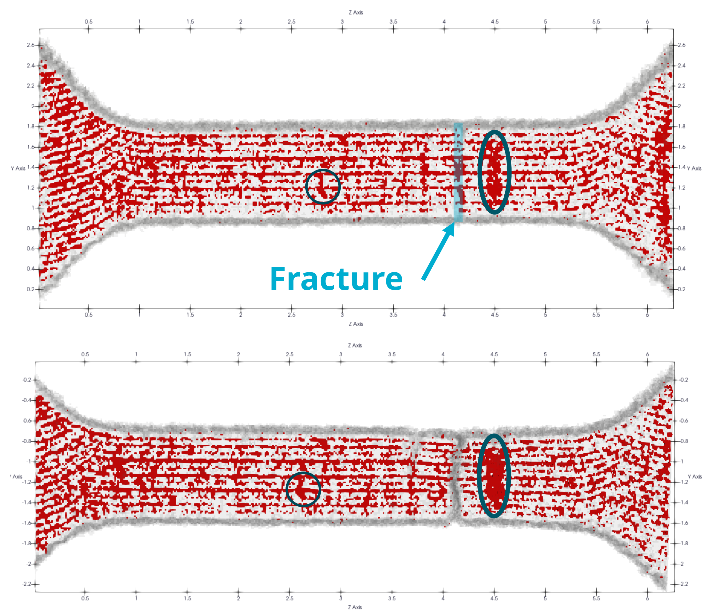

Fracture Location ≈ 4.184 mm

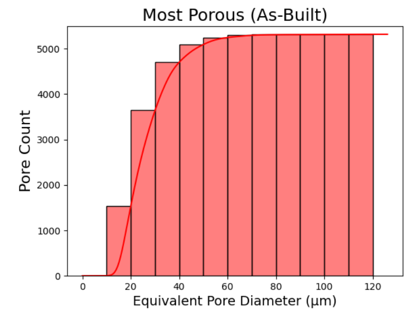

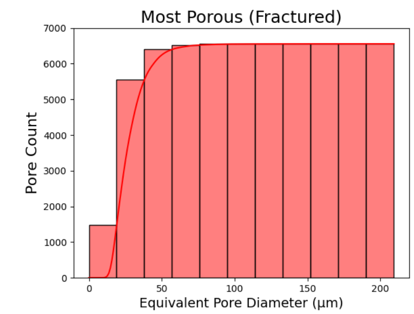

Equivalent diameter 2.29% increase

Stress-strain response – different damage exponent (m)

m ∝ damage

$$\dot{v}_v = \sqrt{\frac{2}{3}}\dot{\varepsilon}_p \frac{1}{\eta}(1+\eta v_v)\left[(1+\eta v_v)^{m+1} - 1\right]$$

$$\cdot \sinh\left[\frac{2(2m-1)}{2m+1}\frac{\langle p \rangle}{\sigma_f}\right] - (v_v - v_0)\frac{\dot{\eta}}{\eta}$$

40 μm voxel size

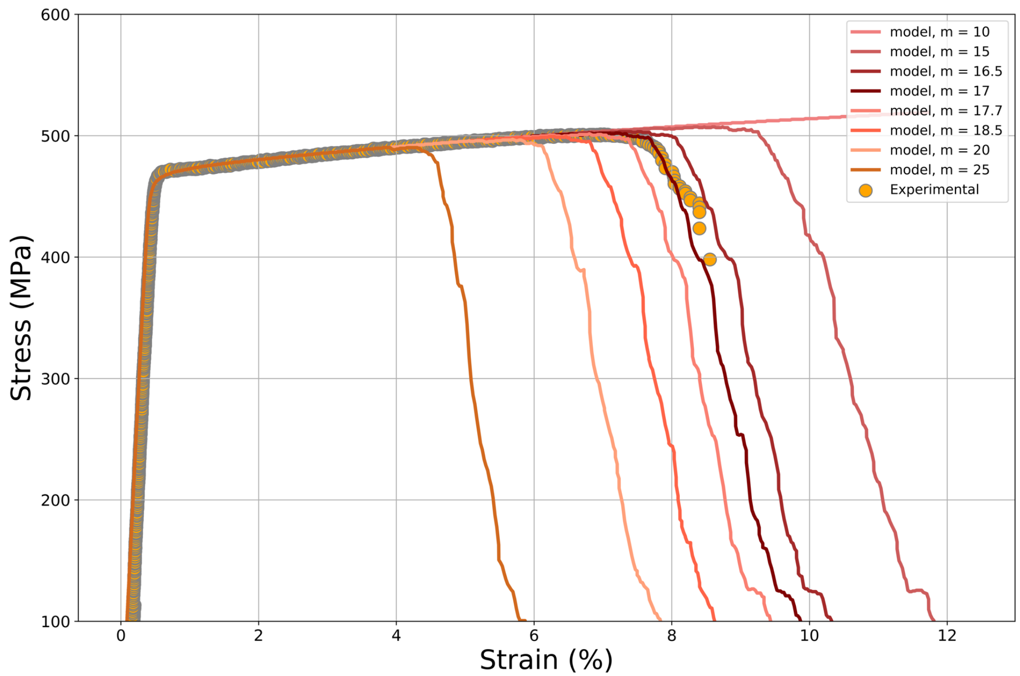

[4]

Cropping volume

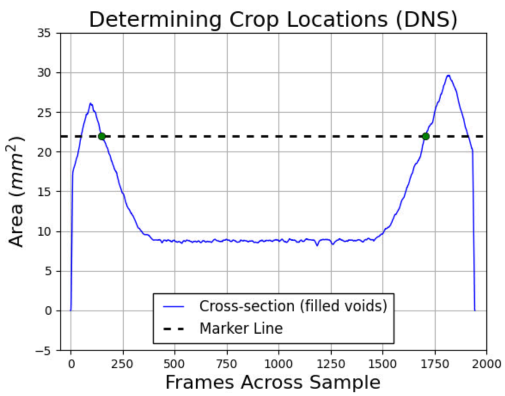

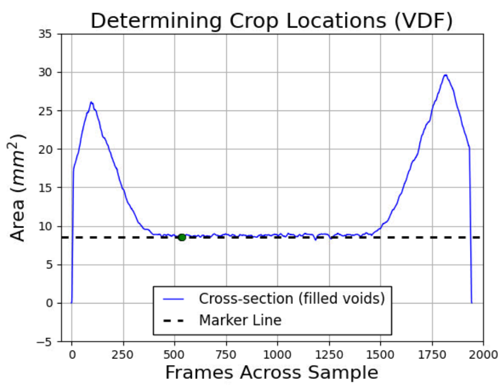

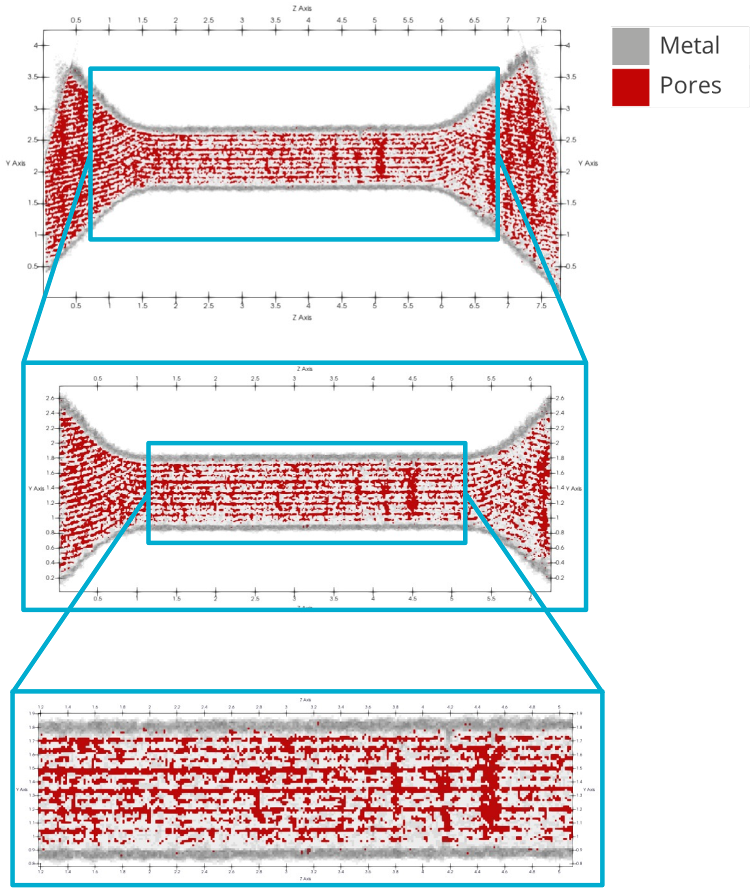

Mesh size effect: porous tensile bar

Porous

80 µm voxel

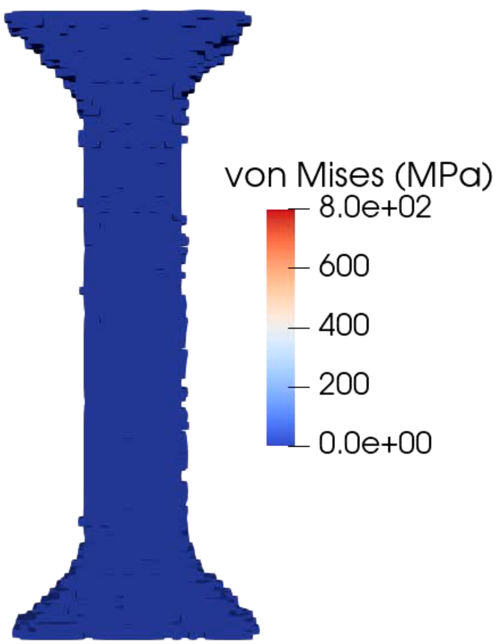

~13k elements
20 processors
0.25 hr wall time

40 µm voxel

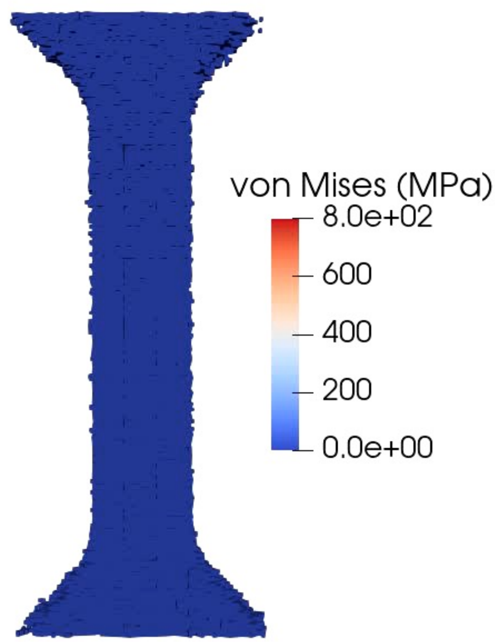

~100k elements
40 processors
1.4 hr wall time

20 µm voxel

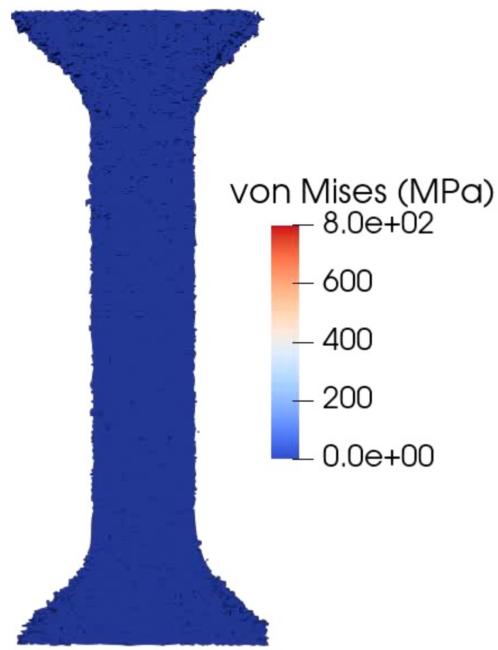

~800k elements
330 processors
2.46 hr wall time

Mesh size effect: most porous tensile bar

Most Porous

80 µm voxel

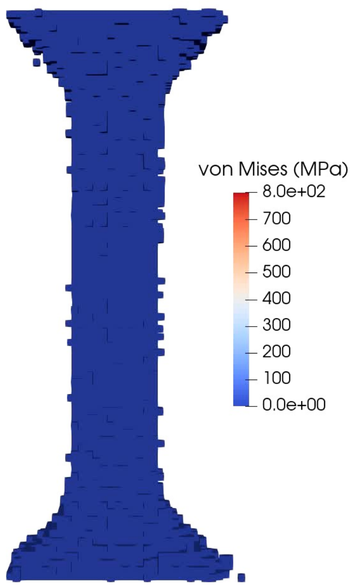

~10k elements

40 µm voxel

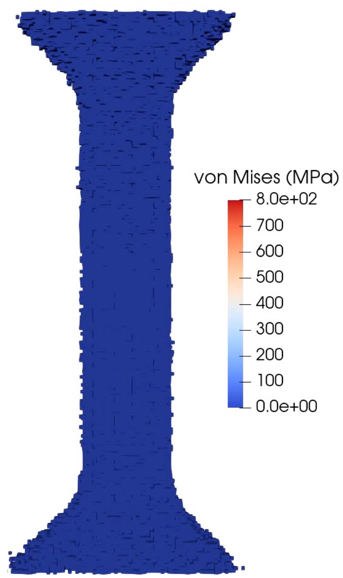

~100k elements

20 µm voxel

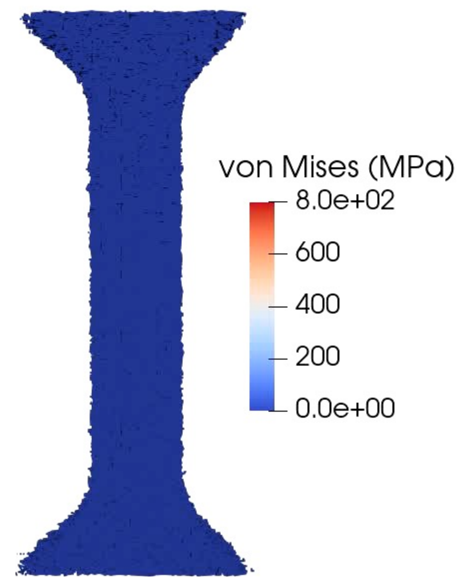

~800k elements